

High definition aperture probes for near-field optical microscopy fabricated by focused ion beam milling

J. A. Veerman,^{a)} A. M. Otter, L. Kuipers, and N. F. van Hulst

Applied Optics group, MESA Research Institute, University of Twente, P.O. Box 217, 7500 AE Enschede, The Netherlands

(Received 5 January 1998; accepted for publication 14 April 1998)

We have improved the optical characteristics of aluminum-coated fiber probes used in near-field scanning optical microscopy by milling with a focused ion beam. This treatment produces a flat-end face free of aluminum grains, containing a well-defined circularly-symmetric aperture with controllable diameter down to 20 nm. The polarization behavior of the tips is circularly symmetric with a polarization ratio exceeding 1:100. The improved imaging characteristics are demonstrated by measuring single molecule fluorescence. Count rates increase more than one order of magnitude over unmodified probes, and the molecule images map a spatial electric field distribution of the aperture in agreement with calculations. © 1998 American Institute of Physics.

[S0003-6951(98)01624-6]

In near-field scanning optical microscopy (NSOM) a high-resolution optical image is obtained by scanning a sub-wavelength light source over the sample surface.^{1,2} Ideally, this light source should combine a high brightness, good polarization characteristics and a small well-defined aperture. The most widely used subwavelength light source consists of a tapered optical fiber obtained by heating and subsequent pulling, which is coated with aluminum to create an aperture smaller than 100 nm.^{2,3} Advantages of these probes are the reproducibility of fabrication, sharpness down to 20 nm, the ease of delivering light to the end of the probe, the flat endpoint being beneficial in NSOM imaging, and the small lateral dimensions of the probe enabling a good access to corrugated samples. Pulled aperture NSOM probes have been applied in a variety of experiments,^{4,5} including single molecule detection.⁶⁻⁸ These probes can have a high degree of polarization in one particular direction^{4,9} (better than 1:20). The optical throughput efficiency of these probes is typically 10^{-6} for a 100 nm probe, but also efficiencies of 10^{-5} have been reported.³ The probe brightness is limited mainly by thermal damage of the aluminum coating to several tens of nanowatts for a 100 nm probe.³ An alternative approach to manufacture NSOM probes is by wet chemical etching.^{10,11} Bare optical fibers are dipped in an etchant solution to produce a taper with a sharp endpoint. As these tapers have a larger cone angle than pulled tapers, the optical throughput can be considerably higher for the same aperture size.

Despite the improvements in NSOM aperture probe fabrication, imperfections in the manufacturing process still limit the quality of aluminum-coated tapered optical fiber probes and their application in nanoscale optical microscopy. First, the evaporated aluminum coating has a grainy structure, including grains at the very end of the probe which decrease the optical imaging capabilities.³ The grains (size 10 nm up to 50 nm) increase the distance between the aperture and the sample which leads to a reduction of both resolution and intensity: the near-field confinement of the light

emerging the probe is lost with increasing distance, and the intensity decays exponentially.^{12,13} Moreover, the grains cause the effective aperture to deviate from an ideal circular shape. Thus, a quantitative interpretation of NSOM images becomes impossible. Second, the polarization behavior of pulled fiber NSOM tips generally is highly asymmetric, which makes it impossible to rotate the linear polarization and at the same time maintain its purity. The degree of linear polarization of the light transmitted by the probe in most cases is only 1:3 for the worst direction. This has been attributed to asymmetric taper shapes and the grainy structure of the aluminum surrounding the aperture.⁹ Third, pinholes at the taper region are easily formed.³ The angled evaporation of the aluminum to leave an aperture at the flat end of the probe induces pinholes through shadowing by dust particles. Pinholes close to the aperture cause a significant loss of light throughput by the aperture. Furthermore, the pinholes disturb the polarization behavior of the tip. Fourth, both optical throughput and maximum brightness of pulled apertured fiber NSOM probes are rather limited, as mentioned above. An additional disadvantage is the dependence of the throughput efficiency on the polarization direction, causing differences up to one order of magnitude. Chemically etched probes have higher throughputs, but they still suffer from the above-mentioned problems caused by the aluminum coating. Furthermore, the very end of these tips is not flat but rounded, which effectively decreases the resolution.

Muranishi *et al.*¹⁴ recently reported aperture fabrication on gold-coated chemically etched NSOM probes by focused ion beam (FIB) slicing, getting apertures down to 100 nm with a fabrication error of 35 nm. Head-on focused ion beam drilling of NSOM probes has been reported by Baida *et al.*¹⁵ and Lacoste *et al.*⁹ We have improved the aperture definition, the polarization behavior and imaging capabilities of fiber NSOM aperture probes using the focused ion beam technique, which is capable of polishing the end of the probe on a nanometer scale. Moreover, we characterize the optical

^{a)}Electronic mail: j.a.veerman@tn.utwente.nl

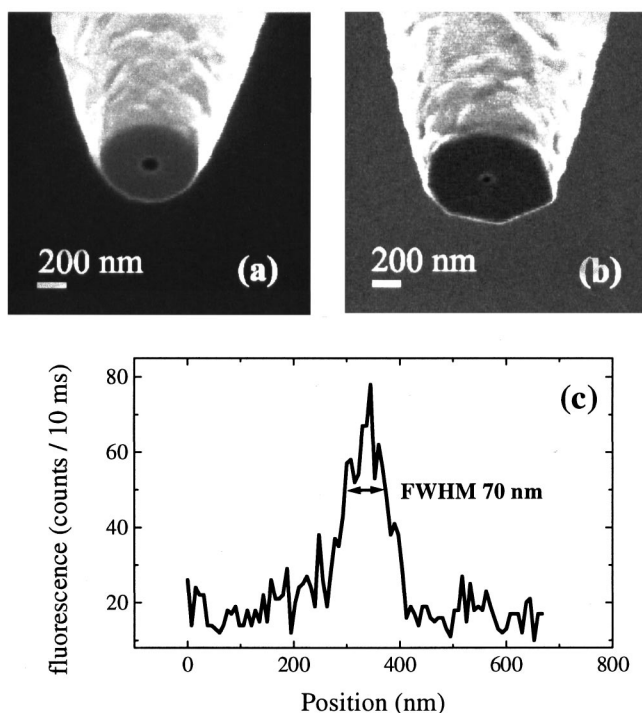


FIG. 1. FIB images of FIB-etched NSOM probes with aperture diameter of (a) 120 nm and (b) 35 nm. (c) Linescan taken with a near-field optical microscope (Ref. 8) using a 60 nm probe of the fluorescence of a single R6G molecule linked to a double stranded DNA molecule deposited on mica, showing a FWHM of 70 nm.

characteristics of the probe by measuring single molecule fluorescence.

Our probe fabrication approach is as follows. First, fiber tips are pulled with a commercial fiber puller (Sutter Instruments P2000). The sharpness of the pulled uncoated tip determines the minimum obtainable aperture size of the finished probe. The probes are coated using e-beam evaporation of aluminum. Evaporation at an angle of approximately 75° with respect to the probe axis creates an aperture, while evaporation at an angle of 90° covers the entire fiber end. After coating the probes are loaded in the FIB machine (FIB 200, FEI). Gallium ions focused to a beam of 10 nm are scanned at 90° with the tip axis, thereby removing a very thin slice of material from the tip end. An existing aperture can thus be flattened, while an entirely coated probe end can be opened. The result is a flat-end face with a roughness smaller than 10 nm and a well-defined circular aperture. The aperture can be made of any desirable diameter, simply by changing the thickness of the slice that is milled. We have been able to make apertures as small as 20 nm with this technique. FIB etching is done at a moderate density of the ion beam (11 pA, 30 kV). Using a low density beam (1 pA), the machine can be used for imaging (like a scanning electron microscope) before and after milling for inspection. The imaging resolution of our apparatus is better than 10 nm and the sample stage drift is less than 10 nm per minute.

Figures 1(a) and 1(b) show images of two FIB-etched tips, showing a flat-end face and well-defined circular aperture of 120 (± 5) nm and 35 (± 5) nm diameter, respectively. Figure 1(c) depicts a line trace of a measurement of the fluorescence of a single R6G molecule deposited on mica.¹⁶ A FWHM of 70 nm is obtained at a scan height of 15

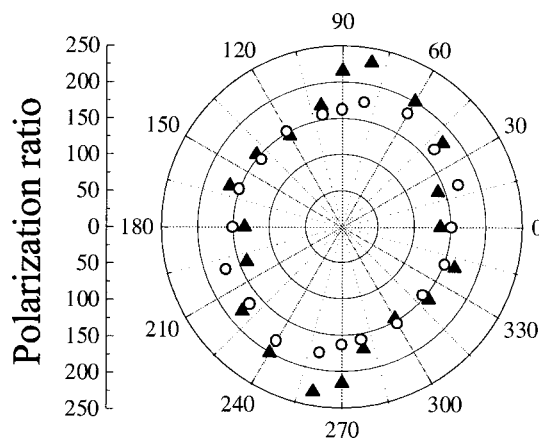


FIG. 2. Polarization ratio (closed triangles) and relative throughput (open circles) as a function of incoming polarization direction for the 35 nm probe shown in Fig. 1(b).

nm, which is in agreement with the aperture diameter of 60 (± 5) nm as determined from the FIB image.

The polarization behavior of our FIB-etched tips was characterized in the far field using a 0.5 NA objective at an optical wavelength of 632.5 nm. The input polarization was controlled using half-wave and quarter-wave plates, while an analyzer before the detector determined the degree of polarization. We find polarization ratios typically exceeding 1:40 for all directions, which is a considerable improvement which respect to probes produced without FIB etching. We have obtained probes with polarization ratios higher than 1:100 for all directions, with maximum ratios up to 1:250. The difference between maximum and minimum polarization ratio is less than a factor of 3. The throughput of FIB-etched probes is usually constant within 20% with the polarization direction. Figure 2 depicts an example of the polarization ratio (triangles) and relative throughput (circles) as a function of polarization direction for the 35 nm aperture probe of Fig. 1(b).

The throughput shows a strong dependence on aperture diameter, ranging from 6×10^{-9} for a 20 nm aperture to 10^{-5} for a 90 nm aperture, respectively. We have observed that probes with the same diameter (as determined in the FIB images) have throughput differences up to one order of magnitude, probably reflecting the influence of the taper shape on the probe efficiency.⁹

It is best not to use transmission contrast for testing the optical imaging capabilities of NSOM probes, as this can easily be affected by sample topography.¹⁷ We characterize our probes by measuring individual fluorescent molecules,^{6-8,16} because a single fluorescent molecule acts as a local detector which maps the optical near-field distribution of the aperture: the overlap between the orientation of the molecular absorption dipole and the electric field polarization at a certain position of the aperture determines the fluorescence intensity of the molecule. Thus, measuring the intensity and polarization behavior of single molecule fluorescence as a function of probe position provides a direct map of the near-field distribution of the NSOM probe.^{6,12,13} This is demonstrated in Figs. 3(a)–3(c) which show three images of one single Perylene Orange molecule deposited on glass and covered by a 20 nm PMMA layer, obtained by

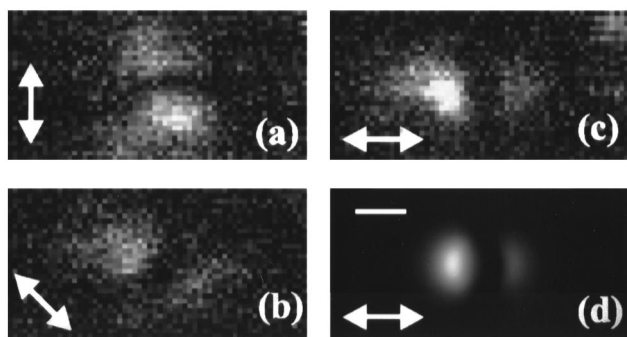


FIG. 3. (a)–(c) Three sequential images of the same molecule (Perylene Orange on glass covered by a 20 nm PMMA layer) for different linear excitation polarization directions (arrows), taken with the 120 nm probe of Fig. 1(a) (pixelsize: 15 nm). (d) Simulation (Ref. 12) of the near-field intensity pattern of a molecule oriented at 15° polar angle and 30° azimuthal angle with respect to the incoming polarization direction (arrow) at 35 nm distance from a 120 nm aperture (scalebar: 150 nm).

scanning the FIB-etched probe of Fig. 1(a) at ~ 15 nm over the sample (pixel size 15 nm). The molecule image consists of two lobes, oriented along the direction of the incoming polarization as measured in the far field (arrows). It is known from calculations^{12,13} that axial electric field components can exist at the rims of the aperture. The calculated intensity pattern for a probe-sample distance of 35 nm, a polar angle of 15° (with respect to the direction perpendicular to the sample plane), an azimuthal angle of 30° (with respect to the horizontal direction in the image) and an excitation polarization along the horizontal direction (arrow) is depicted in Fig. 3(d).¹² This molecule is only excited when it is underneath the rims of the aperture. Changing the direction of the polarization changes the orientation of the lobes, which clearly indicates that the lobes resemble the electric field distribution of the probe mapped by only one molecule, rather than being the fluorescence of two distinct molecules. We have observed such two-lobed shapes for many molecules and with several different probes. This near-field effect is only present at a sharp and well-defined boundary between aperture and coating. It is often obscured in unmodified NSOM probes due to aluminum grains. Probably this is the reason why the early data of Betzig and Chichester⁶ have been difficult to reproduce. Two conclusions can be drawn from these images. First, we are able to image the substructure in the electric field distribution of our probes. Second, the substructure resembles the patterns that are obtained in simulations for circular flat apertures.

The near-field intensity of the light emerging a NSOM probe shows a strong exponential distance dependence. Therefore, in order to maintain the near-field confinement and the maximum intensity, it is important to minimize the distance between probe and sample. The flatness of a FIB probe provides a minimum distance to the sample, which increases not only the resolution but also the emission inten-

sity of the molecules. We have imaged single molecules with a 85 nm FIB probe of intensity higher than 1 kW/cm² obtaining 0.5×10^6 photocounts per second, which is an improvement of one order of magnitude compared to unmodified probes.^{6–8}

We have presented a new method of NSOM tip modification using FIB processing with several advantages. It produces well-defined flat apertures down to 20 nm. It improves the polarization characteristics of the probe to polarization ratios exceeding 1:100 in all directions. Angled evaporation of aluminum is no longer necessary, thereby reducing the occurrence of pinholes on the tapering region. The imaging characteristics improve as the probe end is flattened due to a decrease of the distance between sample and probe. Images of single fluorescent molecules show substructure resembling the electric field distribution of the NSOM probe. Moreover, an improved lateral resolution and a higher molecular emission intensity have been observed. The technique is certainly promising in improving NSOM probes fabricated by other methods than pulling, such as chemical etching and micromechanical machining.

The authors gratefully acknowledge MASER Engineering for the use of the FIB machine. This work was mainly supported by the Dutch organization for fundamental research on matter (FOM).

- ¹D. W. Pohl, W. Denk, and M. Lanz, *Appl. Phys. Lett.* **44**, 651 (1984).
- ²E. Betzig, J. K. Trautman, T. D. Harris, J. S. Weiner, and R. L. Kostelak, *Science* **251**, 1468 (1991).
- ³G. A. Valaskovic, M. Holton, and G. H. Morrison, *Appl. Opt.* **34**, 1215 (1995).
- ⁴D. A. Vanden Bout, J. Kerimo, D. A. Higgins, and P. F. Barbara, *Acc. Chem. Res.* **30**, 204 (1997).
- ⁵M. H. P. Moers, W. H. J. Kalle, A. G. T. Ruiters, J. C. A. G. Wiegant, A. K. Raap, J. Greve, B. G. de Grooth, and N. F. van Hulst, *J. Microsc.* **182**, 40 (1996).
- ⁶E. Betzig and R. Chichester, *Science* **262**, 1422 (1993).
- ⁷X. S. Xie and R. C. Dunn, *Science* **265**, 361 (1994).
- ⁸A. G. T. Ruiters, J. A. Veerman, M. F. Garcia-Parajo, and N. F. van Hulst, *J. Phys. Chem. A* **101**, 7318 (1997).
- ⁹Th. Lacoste, Th. Huser, R. Prioli, and H. Heinzelmann, *Ultramicroscopy* **71**, 333 (1998).
- ¹⁰P. Hoffmann, B. Dutoit, and R.-P. Salathé, *Ultramicroscopy* **61**, 165 (1995).
- ¹¹D. Zeisel, S. Nettesheim, B. Dutoit, and R. Zenobi, *Appl. Phys. Lett.* **68**, 2491 (1996).
- ¹²H. A. Bethe, *Phys. Rev.* **66**, 163 (1944); C. J. Bouwkamp, *Rep. Prog. Phys.* **17**, 35 (1954).
- ¹³L. Novotny, D. W. Pohl, and B. Hecht, *Opt. Lett.* **20**, 970 (1995), and references therein.
- ¹⁴M. Muranishi, K. Sato, S. Hosaka, A. Kikukawa, T. Shintani, and K. Ito, *Jpn. J. Appl. Phys., Part 2* **36**, L942 (1997).
- ¹⁵F. Baida, D. Courjon, and G. Tribillon, in *Near Field Optics*, edited by D. W. Pohl and D. Courjon, NATO ASI Series (Kluwer, Dordrecht, 1993), p. 71.
- ¹⁶M. F. Garcia-Parajo, J. A. Veerman, S. J. T. van Noort, B. G. de Grooth, J. Greve, and N. F. van Hulst, *Bioimaging* **6**, 43 (1998).
- ¹⁷B. Hecht, H. Bielefeldt, Y. Inouye, D. W. Pohl, and L. Novotny, *J. Appl. Phys.* **81**, 2492 (1997).